# Three centuries of winter temperature change on the southeastern Tibetan Plateau and its relationship with the Atlantic Multidecadal Oscillation

**Shiyuan Shi [a], Jinbao Li [b], Jiangfeng Shi [a *], Yesi Zhao [a], Gang Huang [c]**

[a] Ministry of Education Key Laboratory for Coast and Island Development, School of Geographic and Oceanographic Sciences, Nanjing University, Nanjing, 210023, China

[b] Department of Geography, University of Hong Kong, Pokfulam, Hong Kong, China

[c] State Key Laboratory of Numerical Modeling for Atmospheric Sciences and Geophysical Fluid Dynamics, Institute of Atmospheric Physics, Chinese Academy of Sciences, Beijing, 100029, China

[*] Corresponding author at Ministry of Education Key Laboratory for Coast and Island Development, School of Geographic and Oceanographic Sciences, Nanjing University, Nanjing, 210023, China.
*Email address*: shijf@nju.edu.cn (J. Shi)

## Abstract

Long-term, high-resolution proxy records containing cold season temperature signals are scarce on the southeastern Tibetan Plateau (TP), limiting our understanding of regional climate and the potential driving forces. In this study, we present a nearly three centuries long reconstruction of winter (December-February) mean temperature for the central Hengduan Mountains, southeastern TP. The reconstruction is derived from a composite tree-ring width chronology of *Pinus yunnanensis* Franch from two high elevation sites (> 3000 meters above sea level). Our reconstruction passes all standard calibration-verification schemes and explains nearly 73% of the variance of the original instrumental data. However, we were constrained to calibrate our full period (1718-2013) reconstruction of December-February mean temperature on the calibration period from 1959-1992 only, due to a decrease in temperature sensitivity of tree-ring index exhibited after 1992. Spatial correlation analysis shows that our reconstruction represents large-scale temperature variations in southwest China and the eastern TP. Our reconstructed December-February mean temperature shows a close association with the Atlantic Multidecadal Oscillation (AMO) over the past three centuries, with warm (cold) periods coinciding with the positive (negative) phases of the AMO. This persistent relationship suggests that the AMO may have been a key driver of multidecadal winter temperature variations on the southeastern TP.



**Keywords:** Palaeoclimatology • Dendrochronology • Winter temperature • Atlantic Multidecadal Oscillation (AMO) • Southeastern Tibetan Plateau

## 1 Introduction

Climate has been changing dramatically since the early twentieth century (IPCC 2013). Whether recent climate change is unprecedented or still within the range of natural variability is a key scientific question (IPCC 2013, PAGES 2k Network 2013, Tingley and Huybers 2013, Wilson et al. 2016). Annually resolved, precisely dated tree-rings are crucial in this pursuit, as they provide a long-term background for assessing current climate regimes and a target for verifying climate model simulations (Collins et al. 2002; IPCC 2013).

Situated in the southeastern Tibetan Plateau (TP), southwestern China, the Hengduan Mountains are one of the earliest places where dendrochronological studies were carried out in China (Wu and Lin 1983; Wu et al. 1988; Wu and Zhao 1991). During the past decade, tree-ring studies have continued to thrive in this region (e,g., Fan et al. 2008a, b; Fan et al. 2009a, b; Guo et al. 2009; Fan et al. 2010; Fang et al. 2010; Li et al. 2011a, b; Li et al. 2012; Zhao et al. 2012; Bi et al. 2015; Li et al. 2015). This is due in large part to unique biological significance as a world biodiversity hotspot (Myers et al. 2000), abundant forest resources (China Forest Editing Committee 2003), and high sensitivity to global climate change (Baker and Moseley 2007; Li et al. 2009b).

Previous studies revealed that radial tree growth is mainly limited by low temperature at high altitudes and water stress at low altitudes in the Hengduan Mountains (Fan et al. 2009a). Based on these response patterns, temperature reconstructions have been conducted for warm seasons at a few sites across the

southeastern TP (Fan et al. 2009b, 2010; Li et al. 2011b, 2012; Li et al. 2015), and for the whole year in the central Hengduan Mountains (Fan et al. 2008a). Moisture-related reconstructions have been developed in the region as well (Fan et al. 2008b; Fang et al. 2010; Li et al. 2011a; Bi et al. 2015; Li et al. 2016). However, cold season temperature reconstructions are still scarce (Shao and Fan 1999), although significant positive responses of tree growth to winter temperature have been found in a few cases (Fan et al. 2008a; Fan et al. 2009a). Winter chilling damage is one of the major meteorological disasters in southwest China (Xie and Cheng 2004), and thus cold season temperature reconstructions are particularly crucial for understanding the long-term variability and the potential driving forces behind winter chilling damage. To this end, we present a new tree-ring width chronology of *Pinus yunnanensis* Franch, a tree species that has been used less frequently for dendroclimatic research, from two high altitude sites in the Hengduan Mountains, southeastern TP. As shown below, the high sensitivity of the *P. yunnanensis* Franch chronology to winter temperature allows us to develop a reliable reconstruction to perceive regional winter temperature variations during the past three centuries.

## 2 Data and methods

### 2.1 Study area and regional climate

The two sampling sites, Dabaoshi (DBS, 27°46'N, 99°47'E, 3390 m above sea level (a.s.l.)) and Luodize (LDZ, 27°48'N, 99°51'E, 3380 m a.s.l.), are located in Shangri-La, northwestern Yunnan province, southwest China (Fig. 1). This area forms

the hinterland of the Hengduan Mountains on the southeastern TP. The climate of this area is characterized by alternations of the South Asian monsoon in summer and the south branch of the westerlies in winter (Duan 1997). Meteorological data used in this study are from the Shangri-La meteorological station (27°50'N, 99°42'E, 3276.7 m a.s.l.), which is the closest to the sampling sites (Fig. 1). Based on the measurements from 1958 to 2014, the annual mean temperature of Shangri-La is 6.0 °C, with the warmest monthly temperature of 13.7 °C in July and the coldest of −2.9 °C in January (Fig. 2). Annual total precipitation is 628.3 mm. The South Asian summer monsoon causes the warm and moist rainy season from June to October (Duan 1997), with precipitation accounting for more than 80% of the total. The influence of the westerlies causes the dry seasons in this region from November to next May (Duan 1997). All the observed seasonal temperatures show an increasing trend, with winter temperature having the highest rising rate among all seasons and the minimum temperatures increasing faster than the maximum and mean temperature in each season (Fig. 3).

Instrumental winter temperatures from Kunming and Tengchong meteorological stations were used to validate the relationship between tree growth and winter temperature over a longer period (Fig. 1). Kunming and Tengchong meteorological stations have the earliest temperature records in Yunnan province, dating back to 1921 and 1916, respectively (Table S1). Wang (1996) interpolated the missing data and built a continuous series for each station. Winter temperature variations in Kunming and Tengchong are similar to and significantly correlated with that of Shangri-La

during their common period 1959-2013 (Table S1, Fig. S1).

2.2 Tree-ring data

Following standard dendrochronological techniques (Cook and Kairiukstis 1990), we collected tree-ring samples of *P. yunnanensis* Franch from the DBS and LDZ sites in Shangri-La, southeastern TP (Fig. 1, Table 1). All samples were mounted and sanded using standard procedures (Stokes and Smiley 1968). After being visually cross-dated under microscope, each ring width was measured to a precision of 0.001 mm using a LINTAB 5.0 system. The quality of cross-dating was checked by the COFECHA program (Holmes 1983). Eventually, 61 cores from 31 trees of DBS and 56 cores from 29 trees of LDZ were used to develop a composite ring-width chronology.

Each raw series of measurements was detrended using the program RCSigFree (http://www.ldeo.columbia.edu/tree-ring-laboratory/resources/software). Prior to standardization, an initial power transformation was used to reduce heteroscedastic behavior commonly found in tree-rings (Cook and Peters 1997). Conservative detrending with negative exponential curves or linear regression curves of any slope was applied to detrend all series. Age-dependent spline was also applied as an additional detrending method to assess the ability of tree-rings to track recent temperature trends. Ring-width indices were calculated as residuals between actual ring-width and estimated values, and the robust biweight mean was used to assemble the chronology. We applied the "signal-free" approach to reduce potential trend distortion in tree-ring chronologies (Melvin and Briffa 2008). The Rbar weighted

125 method was used for variance stabilization (Osborn et al. 1997). The mean inter-series
126 correlation (Rbar) and the expressed population signal (EPS) were calculated for
127 51-year moving windows (Wigley et al. 1984). We used the EPS with a threshold
128 value of 0.90 to assess the most reliable time span of each chronology.

129 2.3 Methods

130 The relationship between tree growth and climate was explored using Pearson's
131 correlation coefficient. Kalman filter and 21-yr running correlation were applied to
132 further test whether tree growth and climate relationships were time-dependent.
133 Kalman filter was introduced into dendroclimatology to detect time-dependent
134 responses of trees to climate factors because it allows time-dependent regression
135 coefficients for predictors (Visser and Molenaar 1988). The dominant climate factor
136 of tree growth (prior winter temperature in this study) was reconstructed using a linear
137 regression model (Cook and Kairiukstis 1990). Leave-one-out cross-validation
138 method was employed to examine the statistical fidelity of the model due to the
139 shortness of the overlapping period between meteorological data and the tree-ring
140 chronology (Michaelsen 1987). The spatial representativeness of the reconstructed
141 temperature was explored by calculating spatial correlations with the temperature data
142 from $0.5^{o}\times0.5^{o}$ Climate Research Unit (CRU) TS3.23 grids using the KNMI climate
143 explorer (Trouet and van Oldenborgh 2013; Harris et al. 2014). The reconstructed
144 temperature series was also compared with other tree-ring based temperature
145 reconstructions in nearby areas to verify its reliability during the past three centuries.
146 Finally, the reconstructed temperature series was compared with the Atlantic

147 Multidecadal Oscillation (AMO) indices and reconstructions to explore its driving
148 forces.

149 **3 Results and discussion**

150 3.1 Characteristics of tree-ring chronologies

151 A 311-year (1703-2013) and a 276-year (1738-2013) ring-width chronology was
152 developed for DBS and LDZ, respectively (Figs. 4a, b). Comparison between the two
153 chronologies showed that they matched well with each other and had similar statistics
154 (Table 1). Considering the proximity of the two sites (8.3 km in direct distance) and
155 the high correlation ($r = 0.62$, $p < 0.001$) over their common reliable period
156 1754-2013, we pooled all 117 samples to build a composite chronology (hereafter,
157 DBSLDZ), with a reliable period 1718-2013 based on EPS higher than 0.90 (Figs. 4c,
158 d). The mean sensitivity of DBSLDZ was 0.10, a typical value for conifers in humid
159 environments (Fan et al. 2009a). The absent rings accounted for 0.18% of the total.
160 The inter-correlation of raw series was 0.56, indicating strong common signals in the
161 samples.

162 3.2 Climate-tree growth relationships

163 Pearson's correlations were calculated between the composite chronology and
164 climate factors on an 18-month window from prior May to current October for two
165 time periods: 1959-1992 and 1993-2013 (Fig. 5). The division is identified by visual
166 inspection and iterative correlation analyses (D'Arrigo et al. 2004a). Climate factors
167 include monthly mean temperature (Tmean), monthly maximum temperature (Tmax),
168 monthly minimum temperature (Tmin), and monthly total precipitation (Pre). During

the earlier period 1959-1992, the correlation results showed that winter temperature was the key factor limiting radial tree growth. Tree growth responses to Tmean, Tmax and Tmin have a similar pattern, with the highest correlations in the cold season, especially from previous December to current February (Fig. 5a). This relationship indicated that winter temperature was the dominant climate factor limiting radial tree growth. The highest correlation was found between DBSLSZ and December-February mean temperature ($r = 0.85$, $p < 0.001$). Meanwhile, the influence of precipitation on radial growth was rather weak in this period, with only a marginally significant correlation found in current May. The correlation coefficients of the first difference series showed similar patterns to the raw data during this period (Fig. 5c).

During the latter period 1993-2013, however, the strength of the association between DBSLDZ and cold season temperatures declined sharply, and the response of tree growth to precipitation was weak (Fig. 5b). The correlations of the first difference series dropped to be insignificant for cold season temperatures, while the correlations with precipitation remained weak (Fig. 5d). These results suggest that the marginally significant correlations with cold season temperatures during this period were largely due to trend, and prior winter temperature was no longer a controlling factor on tree growth after 1992.

We validated the relationship between tree growth and winter temperature further back in time by using two longer instrumental winter temperature series from Kunming and Tengchong meteorological stations on the southeastern TP (Wang 1996). Winter temperatures recorded at the two stations are coherent with that of Shangri-La

during their common period 1959-2013 (Fig. S1, Table S1). Our ring-width chronology traced the winter temperature variations of the two stations quite well at both low- and high-frequencies before 1993, with an apparent and persistent discrepancy after 1992 (Fig. 6, Table 2). These results provide further support for the stable relationship between tree growth and winter temperature back in time and the unusual nature of their divergence after 1992.

The positive response of tree growth to winter temperature during 1959-1992 could be interpreted in terms of known physiological processes. Under low temperature, ice crystals may form in plant tissues, dehydrating cells and disrupting membranes (Körner 1998; Pallardy 2008). Frozen soil also inhibits water absorption and results in winter desiccation, damaging needles and buds and reducing trees' potential for future growth (Körner 1998; Pallardy 2008). Additionally, low temperature and deep snow cover may lead to later and slower initiation of growth in spring (Fritts 1976), shortening the growing season. In contrast, warm conditions and less physiological injuries are favorable to the synthesization and storage of carbohydrates that could be used for cambium growth of the following year (Gou et al. 2007). Similar response patterns have been reported for many tree species in high-latitude or high-altitude regions around the world (D'Arrigo et al. 1997; Pederson et al. 2004; Liang et al. 2006; Gou et al. 2007; Shi et al. 2010; Chen et al. 2012; Shi et al. 2012). In particular, this appears to be a common phenomenon for radial growth of evergreen conifers at high altitude sites in the Hengduan Mountains (Fan et al. 2008a; Fan et al. 2009a, b; Li et al. 2011b, 2012), and its vicinity such as

213 the western Sichuan Plateau and southeastern Tibet (Shao and Fan 1999; Wu et al.
214 2006; Wang et al. 2014).

215 The loss in temperature sensitivity after 1992 could be a manifestation of the
216 so-called “divergence problem” (D'Arrigo et al. 2008; Büntgen et al. 2009), which has
217 been widely recognized in tree-rings at high northern latitudes (Jacoby and Darrigo
218 1995; Briffa et al. 1998; Büntgen et al. 2008), and may exist at lower latitudes as well
219 (Bräuning and Mantwill 2004; Li et al. 2010; Chen et al. 2015). The divergence has
220 also been noted at several sites on the eastern TP. A loss of temperature sensitivity was
221 found in *Abies faxoniana* and *Cupressus cheniana* in Markang after an abrupt
222 warming in 1995, and the cause was attributed to temperature-induced moisture stress
223 (Guo et al. 2015). The growth-climate relationships of *Abies faxoniana* and *Picea*
224 *purpurea* at different slope aspects in Songpan changed after the rapid warming since
225 1980, and soil moisture stress was likely the cause (Guo et al. 2016). Radial growth of
226 *Abies faxoniana* showed a time-dependent relationship to climate variations in
227 Wolong, and the combination of sunshine time decline and cloud cover increase was
228 considered to suppress tree growth and cause recent divergence (Li et al. 2010).
229 Moreover, the divergence phenomenon occurred at a few sites in the Hengduan
230 Mountains as well (Fan et al. 2008a; Zhao et al. 2012), even though at a less extent
231 and not found at all sites (Li et al. 2012; Li et al. 2015).

232 We examined the possible cause of the divergence from several aspects in this
233 study. First, we checked whether the common signals of tree cores decreased after
234 1992 by calculating a 25-yr running Rbar of raw ring-width series and the

prewhitened series without any detrending (Fig. S2a), and a 25-yr running Rbar of ring-width series detrended by two different standardization methods (Fig. S2b). The Rbar values did not decrease in recent decades, indicating that the samples still contain strong common signals. We divided all the 117 raw ring-width series into several subsets and compared the variations of their arithmetic mean series visually to check if there is any growth divergence between different sampling sites or age-levels (Büntgen et al. 2009). As shown in Fig. S3, the ring-width variations at different subsets are similar during their common periods, suggesting that tree growth of different tree ages or sites was controlled by common environmental factors. Therefore, the cause of divergence should be a common force that influences all the samples regardless of their microenvironments or ages.

Second, we checked the homogeneity of temperature data from the Shangri-La meteorological station and its representativeness of trees' living environment. The data homogeneity was tested by comparing with the China Homogenized Historical Temperature (CHHT) dataset (1951-2004) version 1.0 released by the China Meteorological Administration (Li et al. 2009a), which provides China's most homogeneous surface air temperature series by far (Li et al. 2004). We found no bias between the two temperature datasets. We also compared the Shangri-La temperature observations with regional atmospheric background station during 2006-2012. The latter is located on top of a hill with a high vegetation coverage and low-degree influence of human activities while the former is located inside the town (Fig. S4; Yang 2015). The comparison revealed that their temperature differences could be

explained by lapse rate, thus the Shangri-La records have not been disturbed by local environmental changes, such as urbanization. In addition, we checked the winter temperature series from meteorological stations within a range of 150 km around the sampling sites and their correlations with the tree-ring chronology over the period 1959-1992 (Figs. S4, S5). All the data showed coherent correlation pattern, with that from the Shangri-La station having the highest and most stable positive correlation with tree growth (Fig. S5). Therefore, we consider that the meteorological data from the Shangri-La station represents the trees' living environment quite well.

Third, we checked whether the divergence resulted from the detrending method. We used the age-dependent spline smoothing for curve fit to build a new chronology, keeping other configurations the same as the original conservative detrending method. The curve fitting and signal-free convergence iteration differences were shown in Fig. S6. The negative exponential/linear detrending converges with 5 iterations, suggesting an overall less trend distortion than the age-dependent detrending (9 iterations). Comparison of the two chronologies with winter temperature indicated that the trend divergence still exists even if the stiffer age-dependent detrending was applied (Fig. S7b). The disagreement of year-to-year variations between tree-rings and winter temperature after 1992 cannot be resolved by any detrending method as well (Fig. S7c). These results together indicate that the divergence is not due to a failure of detrending.

Finally, we applied Kalman filter and 21-yr running correlation to explore the time-dependent relationships between tree growth and climate. Table S2 shows the results of Kalman filter analysis between DBSLDZ and monthly temperatures and

monthly total precipitation. Constant regression coefficient solutions were applied to most of the variables, and the changes in regression coefficients were only found in winter temperature (Fig. S8). None of the variables showed increasing tendency in regression coefficients. The results of 21-yr running correlation also suggested that the stable and significant positive correlations between DBSLDZ and winter temperature weakened after 1992, without any other temperature or precipitation variables exerting a strong influence to the level as pre-1993 winter temperature for both raw series and their first differences (Fig. S9). Meanwhile, an increase in May-June precipitation sensitivity starting at about the time of the tree ring divergence from winter temperature was noted with the running correlations between the first differenced series (Fig. S9), suggesting that the early growing season moisture may have become more critical to tree growth. Nonetheless, the evidence for May-June precipitation as the new dominant controlling factor on tree growth is still weak.

In summary, the above analyses indicate that the divergence does exist between tree growth and winter temperature at our sampling sites after 1992, and that this phenomenon was not caused by common causes of divergence such as the inhomogeneity of climatic data, detrending end effect, the aging of trees, and differential response to Tmax and Tmin (D'Arrigo et al. 2008). As a result, it is hard to pinpoint the exact cause of the divergence in our study area at the current stage of our research. This is partly because the phenomenon occurred over a very short period, and partly because the phenomenon may be produced by several interwoven environmental factors.

However, we noticed that the correlation between the first differences of DBSLDZ and May-June precipitation increased to be significantly positive at the 0.05 level at about the time when the correlation with December–February temperature

306 dropped suddenly (Figs. 7, S9). May-June precipitation likely became the new
307 dominant limiting factor of *P. yunnanensis* Franch growth in the study area when the
308 role of winter temperature dropped due to rapid winter temperature increase. However,
309 this conclusion should be accepted with caution, and further sampling of this species
310 in the region and process-based physiological studies are needed to further test this
311 hypothesis.

312 3.3 December-February mean temperature reconstruction

313 We reconstructed the December-February mean temperature for the period
314 1718-2013 using a simple linear regression model based on the calibration period
315 1959-1992, eliminating the recent 21 years from the calibration modeling. This
316 method has sometimes been used when the divergence problem appeared (Jacoby et al.
317 2000; D'Arrigo et al. 2004b; Yonenobu and Eckstein 2006). The reconstruction
318 accounted for 73.0% of the actual temperature variance during 1959-1992.
319 Leave-one-out cross-validation method was used to examine the statistical fidelity of
320 this model due to the shortness of the calibration period (Michaelsen 1987). As shown
321 in Table 3, the correlation coefficient between the actual data and the leave-one-out
322 derived estimates was 0.83 ($p < 0.01$). The reduction of error (RE = 0.70) was highly
323 positive, and the results of the sign-test and product mean test (Pmt) were also
324 statistically significant, further demonstrating the validity of our regression model
325 (Fritts 1976).

326 Comparison of the actual and reconstructed December-February mean
327 temperatures indicated a high consistence until 1992, but the chronology's ability to

328 track temperature variations decreased sharply at both high- and low-frequencies
329 thereafter (Figs. 8a, b), and that their residuals remained negative after 1992 (Fig. 8c).
330 Fig. 8d shows the reconstructed December-February mean temperature over the past
331 three centuries. Cold conditions prevailed in 1731-1737, 1754-1769, 1810-1843,
332 1856-1870, 1903-1919 and 1946-1985, while warm intervals were found in
333 1718-1730, 1770-1788, 1871-1890 and 1922-1945. The mean value of the
334 reconstructed temperature series over 1718-1992 is -2.2 $^{o}$C, and the standard deviation
335 (SD) is 0.7 $^{o}$C. Based on the 1718-1992 mean and SD, extremely warm winters (>
336 mean + 1.5SD) included 1719, 1740, 1746, 1784, 1788, 1826, 1845, 1846, 1873,
337 1931-1933, 1957 and 1991; extremely cold winters (< mean - 1.5SD) were 1732,
338 1733, 1755, 1816, 1817, 1821, 1834, 1836-1840, 1864, 1904, 1905, 1914, 1917, 1962,
339 1963, 1965 and 1983. The winters in 1816-1817 and 1983 were apparently the coldest
340 of the past three centuries, likely due to large tropical eruptions of Mt. Tambora in
341 1815 and Mt. El Chichón (Stothers 1984; add a refrence about El Chichón). In
342 addition, 11 out of the 21 winters after 1992 were identified as extremely warm
343 winters (1999, 2001-2003, 2005, 2006, and 2009-2013) according to observed
344 temperature, which indicated that the most recent two decades, especially the winters
345 after 1998, underwent an unusually persistent warming in the context of the past three
346 centuries (Fig. 8d).
347 3.4 Spatial representativeness of the temperature reconstruction
348 Spatial correlations of the instrumental and reconstructed December-February
349 temperature series and the temperature data from 0.5$^{o}$×0.5$^{o}$ CRU TS3.23 grids over

1959-1992 and 1993-2013 were calculated using the KNMI climate explorer. The results showed that our reconstruction captured large-scale winter temperature variability in southwest China and the eastern TP before 1993 (Fig. 9a, c). Since then, the significance level of the spatial correlations decreased, eventually reaching statistical insignificance (Fig. 9b, d).

To verify the reconstruction and to further test the temperature sensitivity of our tree-ring chronology before 1916, we compared the reconstruction with other tree-ring based temperature reconstructions close to our sampling sites (Fig. 1), including an annual mean temperature reconstruction for the period 1750-2003 using the first principal component of four spruce (*Picea brachytyla*) ring-width chronologies (Fan et al. 2008a), a reconstructed summer (June-August) mean temperature series from 1710-2005 using two *Abies georgei* Orr ring-width chronologies (Li et al. 2011b), an annual mean temperature reconstruction covering the period 984–2009 using ring-width series of *Sabina tibetica* Kom. (Wang et al. 2014), and warm season (April–September) mean temperature variations since 1563 using tree-ring maximum late wood density data from *Picea likiangensis* var. *balfouriana* (Duan and Zhang 2014). It should be noted that the reconstruction of Fan et al. (2008a) was based on residual chronologies, chronologies in which low-order persistence has been removed, while the other three chronologies developed by Li et al. (2011b), Wang et al. (2014) and Duan and Zhang (2014) retained more low-frequency variance due to the use of conservative detrending methods. As shown in Fig. 10, most of the cold and warm periods matched well with each other, and the

correlations were all significant at the 0.01 level. After 1992, tree-ring indices of other chronologies increased along with rising temperatures while our chronology showed an obvious trend discrepancy. These comparisons validate the temperature sensitivity of our chronology before 1916, and indicate that the post-1992 divergence was unusual over the whole reconstruction period. In addition, these reconstructions demonstrate that the period of the 2000s was the warmest over the past three centuries (Fig. S10), consistent with our result and supportive of our hypothesis that the recent extremely high temperatures induced the divergence. We also noticed that the divergence found in our research was larger than the departures between tree rings and climate records observed at the other sites in the Hengduan Mountains (Fan et al. 2008a, 2010; Duan and Zhang 2014). This phenomenon might be related to the unique physiological character of *P. yunnanensis* Franch, which was most sensitive to winter temperature that experienced most rapid increase in recent decades (Fig. 3).

### 3.5 Linkage with the AMO

The AMO represents the alternation of warm and cool phases in North Atlantic sea surface temperatures (SSTs) with a periodicity of roughly 70 years (Kerr 2000). It has a notable linkage with multidecadal climate variability over many regions around the globe, such as the fluctuations of global land surface temperature, precipitation in northeastern Brazil, African Sahel, Europe and North American, and Atlantic hurricanes (Knight et al. 2006; Muller et al. 2013). The coherent temperature fluctuations in North Atlantic and many parts of China have been revealed from observations, model simulations and millennium-long proxy records (Li and Bates

2007; Wang et al. 2009; Wang et al. 2013). According to the observational analysis, a positive relationship between the AMO and land surface air temperature exists in most of China, in particular its western part, and that the influence of the AMO on winter temperature is most significant on the southeastern TP (Fig. 11a, Wang et al. 2009). To investigate whether the AMO may have influenced winter temperature of the study area over a longer period, we compared our reconstruction with one instrumental and two reconstructed AMO series (Kaplan et al. 1998; Gray et al. 2004; Mann et al. 2009).

As shown in Fig. 11b, there is a visual similarity between our reconstruction and the instrumental AMO index at annual to multidecadal timescales during 1856-1992. The correlation between detrended annual series was 0.24, significant at the 0.01 level. The AMO reconstruction of Gray et al. (2004) was developed based on tree-ring records from eastern North America, Europe, Scandinavia, and the Middle East, spanning 1567-1990, while Mann et al. (2009) employed a diverse multi-proxy dataset comprising more than one thousand tree-rings, ice cores, corals, sediments, and other assorted proxy records over the past 1500 years. Our reconstruction showed coherent in-phase fluctuations with the two reconstructed AMO series on multidecadal timescales throughout the past three centuries (Figs. 11c, d). The correlations between these series (both with and without detrending) and their decadal series are all significant at the 0.01 level, as estimated using Monte Carlo simulation tests. This finding is consistent with the study of Wang et al. (2014), however over a different season and a longer period, i.e., the past three centuries. In addition, we

compared other temperature reconstructions from nearby regions (i.e., those shown in Fig. 10) with the reconstructed AMO series in the time range of our reconstruction, and found that they show consistent multidecadal fluctuations (Fig. S11). The decadal variations of the reconstructed temperature and AMO series generally correlated significantly at the 0.05 level (Table S3). The correlations between the temperature reconstruction of Fan et al. (2008a) and the AMO series were relatively low, because the former was developed from residual chronologies and contained little multidecadal fluctuations (Table S3). Dynamic analysis indicated that when the AMO is in warm phase, negative surface air pressure anomalies will form, extending from the mid-latitude North Atlantic to the middle-latitude Eurasia. The anomalous air circulation weakens the Mongolian high and cold air activity, inducing a warmer winter over East Asia (Li et al. 2007; Wang et al. 2009; Wang et al. 2013). Together, these studies suggest that the AMO might have been an important forcing on multidecadal temperature variability on the southeastern TP.

## 4 Conclusion

A 296-year robust tree-ring width chronology of *P. yunnanensis* Franch was developed from two high altitude sites in Shangri-La, southeastern TP. The chronology was used to reconstruct December-February mean temperature with an explained variance of 73.0% over the calibration period 1959-1992. The reconstruction revealed that cold conditions prevailed in 1731-1737, 1754-1769, 1810-1843, 1856-1870, 1903-1919, and 1946-1985, while warm intervals were found in 1718-1730, 1770-1788, 1871-1890, and 1922-1945. The reconstruction represents

large-scale winter temperature variations in southwest China and eastern TP. The AMO was shown to be an important forcing of winter temperature change in southwest China over the past three centuries. The period of 2000-2013 was unusually warm during the past three centuries. However, it should be accepted with caution because of the unresolved divergence problem since 1992. Further sampling of this and other tree species in the area and process-based physiological studies should be carried out in order to fully understand the divergence problem and to predict the response of regional forest ecosystem to global warming.

**Acknowledgements**

The authors thank Yanwu Shi and Lingling Li for their help in the laboratory, Bao Yang, Jianping Duan, Zexin Fan and Zongshan Li for sharing their reconstructed temperature data, Jade d'Alpoim Guedes for improving the language, and three anonymous reviewers for their constructive comments. This research was funded by the Research Grants Council of Hong Kong (No. 27300514), the National Science Foundation of China (No. 41271210), the National Key R&D program of China (No. 2016YFA0600503), the Priority Academic Program Development of Jiangsu Higher Education Institutions, and the Jiangsu Collaborative Innovation Center for Climate Change.

## References


Büntgen U, Frank D, Wilson R, Carrer M, Urbinati C, Esper J (2008) Testing for tree-ring divergence in the European Alps. Global Change Biology 14:2443-2453. doi:10.1111/j.1365-2486.2008.01640.x

Büntgen U, Wilson R, Wilmking M, Niedzwiedz T, Bräuning A (2009) The 'divergence problem' in tree-ring research. TRACE - Tree Rings in Archaeology, Climatology and Ecology 7:212-219

Baker BB, Moseley RK (2007) Advancing treeline and retreating glaciers: implications for conservation in Yunnan, P.R. China. Arctic, Antarctic, and Alpine Research 2:200-209. doi:10.1657/1523-0430(2007)39[200:atargi]2.0.co;2

Bi Y, Xu J, Gebrekirstos A, Guo L, Zhao M, Liang E, Yang X (2015) Assessing drought variability since 1650 AD from tree-rings on the Jade Dragon Snow Mountain, southwest China. International Journal of Climatology 35:4057–4065

Bräuning A, Mantwill B (2004) Summer temperature and summer monsoon history on the Tibetan plateau during the last 400 years recorded by tree rings. Geophysical Research Letters 31. doi:10.1029/2004gl020793

Briffa KR, Schweingruber FH, Jones PD, Osborn TJ, Shiyatov SG, Vaganov EA (1998) Reduced sensitivity of recent tree-growth to temperature at high northern latitudes. Nature 391:678-682

Chen F, Yuan Y-j, Wei W-s, Yu S-l, Zhang T-w (2012) Tree ring-based winter temperature reconstruction for Changting, Fujian, subtropical region of Southeast China, since 1850: linkages to the Pacific Ocean. Theoretical and Applied Climatology 109:141-151. doi:10.1007/s00704-011-0563-0

Chen F, Yuan Y, Wei W, Zhang T, Shang H, Yu S (2015) Divergent response of tree-ring width and maximum latewood density of *Abies faxoniana* to warming trends at the timberline of the western Qinling Mountains and northeastern Tibetan Plateau, China. Silva Fennica 49. doi:10.14214/sf.1155China Forest Editing Committee (ed) (2003) China forest: Coniferous forests vol 2. China Forestry Publishing House, Beijing (in Chinese)

Collins M, Osborn TJ, Tett SFB, Briffa KR, Schweingruber FH (2002) A comparison of the variability of a climate model with paleotemperature estimates from a network of tree-ring densities. Journal of Climate 15:1497-1515

Cook ER, Kairiukstis L (1990) Methods of dendrochronology: Applications in the environmental sciences. Springer, New York

Cook ER, Peters K (1997) Calculating unbiased tree-ring indices for the study of climatic and environmental change. The Holocene 7:361-370

D'Arrigo RD, Yamaguchi DK, Wiles GC, Jacoby GD, Osawa A, Lawrence DM (1997) A kashiwa oak (*Quercus dentata*) tree-ring width chronology from northern coastal Hokkaido, Japan. Canadian Journal of Forest Research 27:613-617

D'Arrigo RD, Kaufmann RK, Davi N, Jacoby GC, Laskowski C, Myneni RB, Cherubini P (2004a) Thresholds for warming-induced growth decline at elevational tree line in the Yukon Territory, Canada. Global Biogeochemical Cycles 18:GB3021. doi:3010.1029/2004GB002249

D'Arrigo R, Mashig E, Frank D, Jacoby G, Wilson R (2004b) Reconstructed warm season temperatures for Nome, Seward Peninsula, Alaska. Geophysical Research Letters 31, L09202. doi:10.1029/2004gl019756

D'Arrigo R, Wilson R, Liepert B, Cherubini P (2008) On the 'Divergence Problem' in northern forests:

A review of the tree-ring evidence and possible causes. Global and Planetary Change 60:289-305. doi:10.1016/j.gloplacha.2007.03.004

Duan J, Zhang QB (2014) A 449 year warm season temperature reconstruction in the southeastern Tibetan Plateau and its relation to solar activity. Palaeogeography Palaeoclimatology Palaeoecology 119:215-240

Duan Z (1997) Zhongdian chronicles. The Nationalities Publishing House of Yunnan, Kunming (in Chinese)

Fan Z-X, Bräuning A, Cao K-F (2008a) Annual temperature reconstruction in the central Hengduan Mountains, China, as deduced from tree rings. Dendrochronologia 26:97-107. doi:10.1016/j.dendro.2008.01.003

Fan Z-X, Bräuning A, Cao K-F (2008b) Tree-ring based drought reconstruction in the central Hengduan Mountains region (China) since A.D. 1655. International Journal of Climatology 28:1879-1887. doi:10.1002/joc.1689

Fan Z-X, Bräuning A, Cao K-F, Zhu S-D (2009a) Growth–climate responses of high-elevation conifers in the central Hengduan Mountains, southwestern China. Forest Ecology and Management 258:306-313. doi:10.1016/j.foreco.2009.04.017

Fan Z-X, Bräuning A, Tian Q-H, Yang B, Cao K-F (2010) Tree ring recorded May–August temperature variations since A.D. 1585 in the Gaoligong Mountains, southeastern Tibetan Plateau. Palaeogeography, Palaeoclimatology, Palaeoecology 296:94-102. doi:10.1016/j.palaeo.2010.06.017

Fan Z-X, Bräuning A, Yang B, Cao K-F (2009b) Tree ring density-based summer temperature reconstruction for the central Hengduan Mountains in southern China. Global and Planetary Change 65:1-11. doi:10.1016/j.gloplacha.2008.10.001

Fang K et al. (2010) Reconstructed droughts for the southeastern Tibetan Plateau over the past 568 years and its linkages to the Pacific and Atlantic Ocean climate variability. Climate Dynamics 35:577-585. doi:10.1007/s00382-009-0636-2

Fritts HC (1976) Tree rings and climate. Academic Press, London

Gou X, Chen F, Jacoby G, Cook E, Yang M, Peng H, Zhang Y (2007) Rapid tree growth with respect to the last 400 years in response to climate warming, northeastern Tibetan Plateau. International Journal of Climatology 27:1497-1503. doi:10.1002/joc.1480

Gray ST, Graumlich LJ, Betancourt JL, Pederson GT (2004) A tree-ring based reconstruction of the Atlantic Multidecadal Oscillation since 1567 A.D. Geophysical Research Letters 31. doi:10.1029/2004gl019932

Guo G, Li Z-S, Zhang Q-B, Ma K-P, Mu C (2009) Dendroclimatological studies of *Picea likiangensis* and *Tsuga dumosa* in Lijiang, China. Iawa Journal 30:435-441

Guo B, Zhang Y, Wang X (2016) Response of *Picea purpurea* and *Abies faxoniana* tree rings at different slope aspects to rapid warming in western Sichuan, China. Chinese Journal of Applied Ecology 27: 354-364. doi:10.13287 /j.1001-9332.201602.034

Guo M M, Zhang Y D, Wang X C, Huang Q, Yang S X, Liu S R (2015) Effects of abrupt warming on main conifer tree rings in Markang, Sichuan, China. Acta Ecologica Sinica 35: 7464-7474. doi: 10.5846 /stxb201404140715

Harris I et al. (2014) Updated high-resolution grids of monthly climatic observations–the CRU TS3. 10 Dataset. International Journal of Climatology 34: 623-642

Holmes RL (1983) Computer-assisted quality control in tree-ring dating and measurement. Tree-Ring

544 Bulletin 43:69-78
545 IPCC (2013) Climate Change 2013: The physical science basis. Cambridge University Press,
546 Cambridge, United Kingdom and New York, NY, USA. doi:10.1017/CBO9781107415324
547 Jacoby GC, Darrigo RD (1995) Tree-ring width and density evidence of climatic and potential forest
548 change in Alaska. Global Biogeochemical Cycles 9:227-234. doi:10.1029/95gb00321
549 Jacoby GC, Lovelius NV, Shumilov OI, Raspopov OM, Karbainov JM, Frank DC (2000) Long-term
550 temperature trends and tree growth in the Taymir region of northern Siberia. Quaternary
551 Research 53:312-318
552 Körner C (1998) A re-assessment of high elevation treeline positions and their explanation. Oecologia
553 115:445-459
554 Kaplan A, Cane MA, Kushnir Y, Clement AC, Blumenthal MB, Rajagopalan B (1998) Analyses of
555 global sea surface temperature 1856–1991. Journal of Geophysical Research: Oceans
556 103:18567-18589. doi:10.1029/97jc01736
557 Kerr RA (2000) A North Atlantic climate pacemaker for the centuries. Science 288:1984-1986.
558 doi:10.1126/science.288.5473.1984
559 Knight JR, Folland CK, Scaife AA (2006) Climate impacts of the Atlantic Multidecadal Oscillation.
560 Geophysical Research Letters 33. doi:10.1029/2006gl026242
561 Li J, Shi J, Zhang DD, Yang B, Fang K, Yue PH (2016) Moisture increase in response to high-altitude
562 warming evidenced by tree-rings on the southeastern Tibetan Plateau. Climate Dynamics.
563 doi:10.1007/s00382-016-3101-z
564 Li M-Y, Wang L, Fan Z-X, Shen C-C (2015) Tree-ring density inferred late summer temperature
565 variability over the past three centuries in the Gaoligong Mountains, southeastern Tibetan
566 Plateau. Palaeogeography, Palaeoclimatology, Palaeoecology 422:57-64.
567 doi:10.1016/j.palaeo.2015.01.003
568 Li Q, Liu X, Zhang H (2004) Detecting and adjusting temporal inhomogeneity in Chinese mean surface
569 air temperature data. Advances in Atmospheric Sciences 21: 260-268
570 Li Q, Zhang H, Liu X, Chen J, Li W, Jones P (2009a) A mainland China Homogenized Historical
571 Temperature Dataset of 1951–2004. Bulletin of the American Meteorological Society
572 90:1062-1065. doi:10.1175/2009BAMS2736.1
573 Li S, Bates GT (2007) Influence of the Atlantic Multidecadal Oscillation on the winter climate of East
574 China. Advances in Atmospheric Sciences 24:126-135. doi:10.1007/s00376-007-0126-6
575 Li Z-S, Liu G-H, Fu B-J, Zhang Q-B, Hu C-J, Luo S-Z (2010) Evaluation of temporal stability in tree
576 growth-climate response in Wolong National Natural Reserve, western Sichuan, China.
577 Chinese Journal of Plant Ecology 34:1045-1057. doi:10.3773/j.issn.1005-264x.2010.09.005
578 (in Chinese, with English abstract)
579 Li Z-S, Zhang Q-B, Ma K (2012) Tree-ring reconstruction of summer temperature for A.D. 1475–2003
580 in the central Hengduan Mountains, Northwestern Yunnan, China. Climatic Change
581 110:455-467. doi:10.1007/s10584-011-0111-z
582 Li Z et al. (2009b) Changes of some monsoonal temperate glaciers in Hengduan Mountains region
583 during 1900-2007. Acta Geographica Sinica 64:1319-1330 (in Chinese, with English abstract)
584 Li Z, Shi C, Liu Y, Zhang J, Zhang Q, Ma K (2011a) Winter drought variations based on tree-ring data
585 in Gaoligong Mountain, northwestern Yunnan, China, A. D. 1795-2004. Pakistan Journal of
586 Botany 43:2469-2478
587 Li Z, Shi CM, Liu Y, Zhang J, Zhang Q, Ma K (2011b) Summer mean temperature variation from

588 1710-2005 inferred from tree-ring data of the Baimang Snow Mountains, northwestern
589 Yunnan, China. Climate Research 47:207-218. doi:10.3354/cr01012
590 Liang E, Shao X, Eckstein D, Huang L, Liu X (2006) Topography- and species-dependent growth
591 responses of *Sabina przewalskii* and *Picea crassifolia* to climate on the northeast Tibetan
592 Plateau. Forest Ecology and Management 236:268-277. doi:10.1016/j.foreco.2006.09.016
593 Mann ME et al. (2009) Global signatures and dynamical origins of the Little Ice Age and Medieval
594 Climate Anomaly. Science 326:1256-1260. doi:10.1126/science.1177303
595 Melvin TM, Briffa KR (2008) A "signal-free" approach to dendroclimatic standardisation.
596 Dendrochronologia 26:71-86Michaelsen J (1987) Cross-validation in statistical climate
597 forecast model. Journal of Climate and Applied Meteorology 26:1589-1600.
598 doi:10.1175/1520-0450(1987)026<1589:cviscf>2.0.co;2
599 Muller RA et al. (2013) Decadal variations in the global atmospheric land temperatures. Journal of
600 Geophysical Research: Atmospheres 118:5280-5286. doi:10.1002/jgrd.50458
601 Myers N, Mittermeier RA, Mittermeier CG, Da Fonseca G, Kent J (2000) Biodiversity hotspots for
602 conservation priorities. Nature 403:853-858. doi:10.1038/35002501
603 Osborn T, Briffa K, Jones P (1997) Adjusting variance for sample size in tree-ring chronologies and
604 other regional mean timeseries. Dendrochronologia 15:89-99
605 PAGES 2K Network (2013) Continental-scale temperature variabilityduring the past two millennia.
606 Nature Geoscience 6:339-346. doi:10.1038/NGEO1797
607 Pallardy SG (2008) Physiology of woody plants. 3rd edn. Academic Press, Burlington, San Diego,
608 London
609 Pederson N, Cook ER, Jacoby GC, Peteet DM, Griffin KL (2004) The influence of winter temperatures
610 on the annual radial growth of six northern range margin tree species. Dendrochronologia
611 22:7-29. doi:10.1016/j.dendro.2004.09.005
612 Shao X, Fan J (1999) Past climate on west Sichuan Plateau as reconstructed from ring-width of dragon
613 spruce. Quaternary Sciences:81-89 (in Chinese, with English abstract)
614 Shi J, Li J, Cook ER, Zhang X, Lu H (2012) Growth response of *Pinus tabulaeformis* to climate along
615 an elevation gradient in the eastern Qinling Mountains, central China. Climate Research
616 53:157-167. doi:10.3354/cr01098
617 Shi JF, Cook ER, Lu HY, Li JB, Wright WE, Li SF (2010) Tree-ring based winter temperature
618 reconstruction for the lower reaches of the Yangtze River in southeast China. Climate
619 Research 41:169-175. doi:10.3354/cr00851
620 Stokes MA, Smiley TL (1968) Introduction to tree-ring dating. University of Chicago Press, Chicago
621 Tingley M P, Huybers P (2013) Recent temperature extremes at high northern latitudes unprecedented
622 in the past 600 years. Nature 496: 201-205.doi:10.1038/nature11969
623 Trouet V, van Oldenborgh GJ (2013) KNMI Climate Explorer: A web-based research tool for
624 high-resolution paleoclimatology. Tree-Ring Research 69:3-13. doi:10.3959/1536-1098-69.1.3
625 Visser H, Molenaar J (1988) Kalman filter analysis in dendroclimatology. Biometrics 44:929-940Wang
626 J, Yang B, Ljungqvist FC, Zhao Y (2013) The relationship between the Atlantic Multidecadal
627 Oscillation and temperature variability in China during the last millennium. Journal of
628 Quaternary Science 28:653-658. doi:10.1002/jqs.2658
629 Wang J, Yang B, Qin C, Kang S, He M, Wang Z (2014) Tree-ring inferred annual mean temperature
630 variations on the southeastern Tibetan Plateau during the last millennium and their
631 relationships with the Atlantic Multidecadal Oscillation. Climate Dynamics 43:627-640.

doi:10.1007/s00382-013-1802-0
Wang Y, Li S, Luo D (2009) Seasonal response of Asian Monsoonal climate to the Atlantic Multidecadal Oscillation. Journal of Geophysical Research 114. doi:10.1029/2008jd010929
Wigley T, Briffa KR, Jones PD (1984) On the average value of correlated time-series, with applications in dendroclimatology and hydrometeorology. Journal of Climate and Applied Meteorology 23:201-213. doi:10.1175/1520-0450(1984)023<0201:otavoc>2.0.co;2
Wilson et al. (2016) Last millennium northern hemisphere summer temperatures from tree rings: Part I: The long term context. Quaternary Science Reviews 134: 1-18. doi:10.1016/j.quascirev.2015.12.005
Wu P, Wang L, Huang L (2006) A preliminary study on the tree-ring sensitivity to climate change of five endemic conifer species in China. Geographical Research 25:43-52 (in Chinese, with English abstract)
Wu X, Lin Z (1983) The climatic change and tree-ring analysis in the Hsiao Zhongdian area of the Yunnan province. In: Special issue of Hengduan Mountains scientific expedition, vol 1. The Peoples Press of Yunnan, Kunming, pp 206-213 (in Chinese, with English abstract)
Wu X, Lin Z, Sun L (1988) A preliminary study on the climatic change of the Hengduan Mountains area since 1600 A.D. Advances in Atmospheric Sciences 5:437-443. doi:10.1007/BF02656789
Wu X, Zhao Z (1991) Tree-ring width and climatic change in china. Quaternary Science Reviews 10:545-549
Xie M-E, Cheng J-G (2004) Characteristics and formation mechanism of weather disasters in Yunnan Province. Scientia Geographica Sinica 24:721-726 (in Chinese, with English abstract)
Yang Z (2015) Shangri-La regional atmospheric background station and Shangri-La County AWS ground data analyzed. Henan Science and Technology 10: 145-149 (in Chinease, with English abstract)
Yonenobu H, Eckstein D (2006) Reconstruction of early spring temperature for central Japan from the tree-ring widths of Hinoki cypress and its verification by other proxy records. Geophysical Research Letters 33. doi:10.1029/2006gl026170
Zhao Z, Tan L, Kang D, Liu Q, Li J (2012) Responses of *Picea likiangensis* radial growth to climate change in the Small Zhongdian area of Yunnan Province, Southwest China. Chinese Journal of Applied Ecology 23:603-609 (in Chinese with English abstract)

**Figure Captions:**

**Fig. 1** Location of the sampling sites, the Shangri-La, Kunming and Tengchong meteorological stations, and the sampling sites of Fan et al. (2008a), Li et al. (2011b), Wang et al. (2014), and Duan and Zhang (2014)

**Fig. 2** Monthly mean (Tmean), maximum (Tmax), minimum (Tmin) temperatures, and monthly total precipitation (Pre) from the Shangri-La meteorological station over the period 1958-2014

**Fig. 3** Temporal changes of seasonal mean, maximum and minimum temperatures (line), and total precipitation (gray bar) in (**a**) December-February, (**b**) March-May, (**c**) June-August, and (**d**) September-November over the period 1959-2014

**Fig. 4** (**a**)-(**c**) Tree-ring width chronologies of *Pinus yunnanensis* Franch from two sampling sites, the composite chronology (line), and their corresponding sample depth (gray shading), (**d**) the running Rbar and EPS statistics of the composite chronology. Horizontal dashed line denotes the 0.90 EPS cutoff value

**Fig. 5** Correlation coefficients between DBSLDZ chronology and monthly mean, maximum, minimum temperature and monthly total precipitation. The correlations were calculated between (**a**, **b**) raw series and (**c**, **d**) their first differences over the period (**a**, **c**) 1959-1992 and (**b**, **d**) 1993-2013. The horizontal dashed and dotted lines denote the 95% and 99% confidence level, respectively

**Fig. 6** Comparison of DBSLDZ and the instrumental winter temperature of (**a**) Kunming, and (**b**) Tengchong over the period 1916-2013. All series have been standardized over 1921-1992 for direct comparison

**Fig. 7** The 21-yr running correlations of DBSLDZ with December-February mean temperature and their first differences, and with May-June precipitation and their first differences (every point denotes the last year of a 21-year interval). The horizontal dotted line denotes the 95% confidence level

**Fig. 8** December-February mean temperature reconstruction. (**a**) Comparison of the instrumental (black line) and reconstructed (gray line) temperature during their common period 1959-2013, (**b**) comparison of their first differences, (**c**) residuals of the reconstructed minus instrumental temperature (gray shading), and (**d**) the reconstructed temperature from 1718-1992 (thin black line), its 10-year Fast Fourier Transformation (FFT) smoothing (bold black line), the mean (horizontal solid line) and ±1.5 standard deviation (SD, horizontal dotted line) of the reconstructed temperature series over 1718-1992, and the instrumental data from 1959-2013 (thin red line)

**Fig. 9** Spatial correlations of (**a**, **b**) instrumental and (**c**, **d**) reconstructed December-February temperature series with the CRU TS3.23 land temperature over (**a**, **c**) 1959-1992 and (**b**, **d**) 1993-2013. All series have been detrended prior to spatial correlations. Insignificant correlations ($p \geq 0.1$) are masked out. The blue dot denotes the sampling site

**Fig. 10** Comparison of the reconstructed December-February mean temperature with four tree-ring based temperature reconstructions in the nearby regions. (**a**) The reconstructed December-February mean temperature from this study, (**b**) the annual mean temperature reconstruction in the central Hengduan Mountains (Fan et al. 2008a), (**c**) the June-August mean temperature reconstruction in the Baimang Snow Mountains (Li et al. 2011b), (**d**) the annual mean temperature reconstruction on the southeastern TP (Wang et al. 2014), and (**e**) the April–September mean temperature reconstruction on the southeastern TP (Duan and Zhang 2014). All series were standardized over their common period 1750-1992, and the bold lines denote the 10-year FFT smoothing. Gray bars denote their common cold period, and the blue bar denotes the divergence period 1993-2013

**Fig. 11** The influence of the AMO on winter temperature in the study area. (**a**) Spatial correlation of the AMO with winter land surface temperature from the CRU TS3.23 over 1958-2013. (**b**)-(**d**) Comparison of the reconstructed December-February mean temperature with the AMO series. Black line in (**b**)-(**d**) denotes the reconstructed December-February mean temperature from this study (thin line) and its 11-year moving average (bold line). Red line: (**b**) instrumental AMO index series from Kaplan et al. (1998) (thin line) and its 11-year moving average (bold line), (**c**) the reconstructed AMO index series from Gray et al. (2004) (thin line) and its 11-year moving average (bold line), and (**d**) the reconstructed decadal AMO index series from Mann et al. (2009) (bold line). The series used for comparison were standardized over their common period (**b**) 1856-1992, (**c**) 1718-1990, and (**d**) 1718-1992. Correlations between them are shown in each panel. Single (double) asterisk denotes the correlation significant at 95% (99%) confidence level, respectively

**Table Captions:**

**Table 1** Site information and tree-ring chronology statistics

**Table 2** Correlations of the DBSLDZ chronology with Kunming and Tengchong winter temperature for raw series and their first differences

**Table 3** Statistics of the leave-one-out calibration results for the common period 1959-1992

752 Fig. 1

753

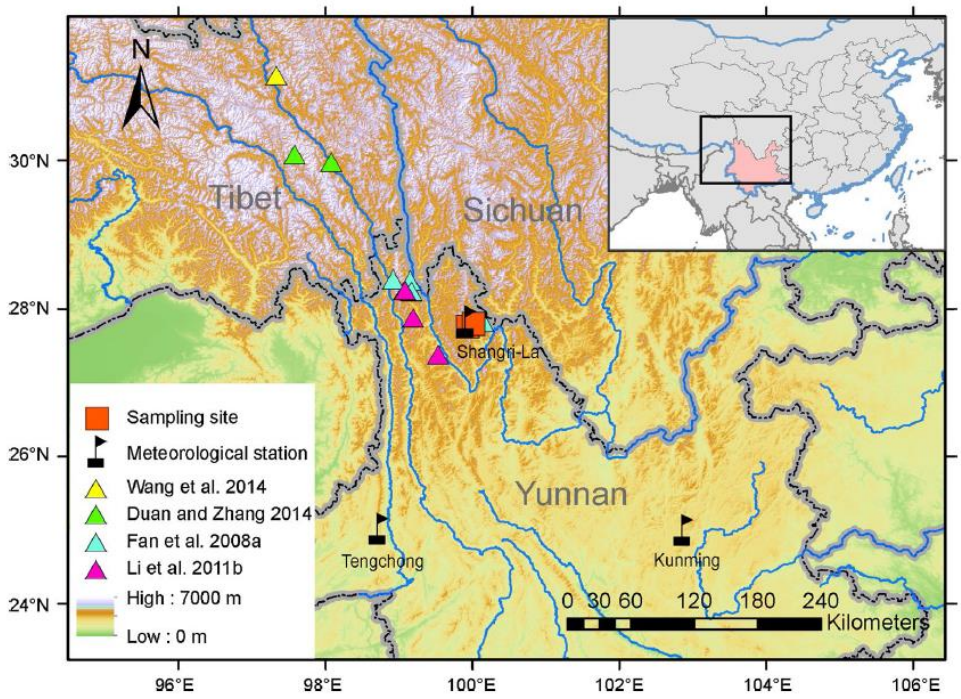


754

755

Fig. 2

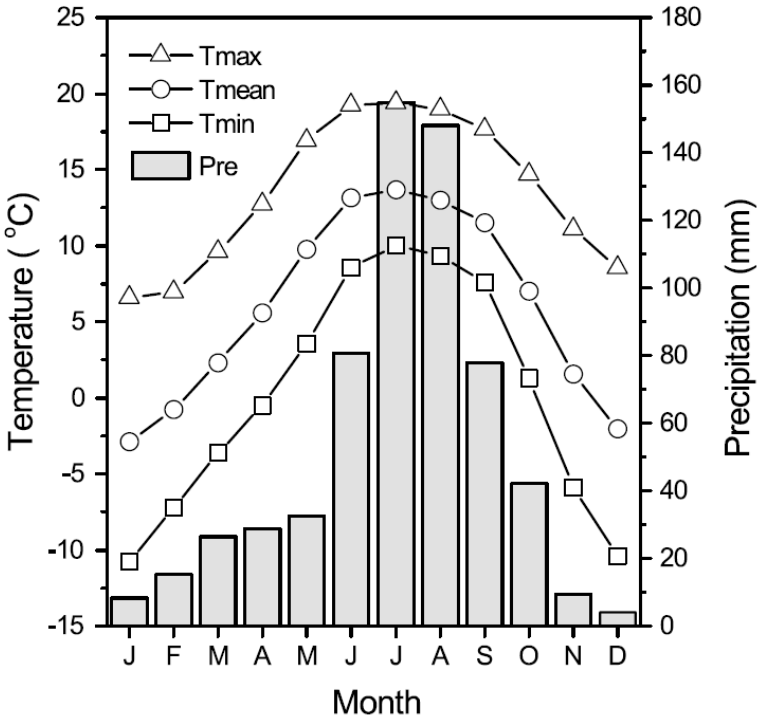
Tmax
Tmean
Tmin
Pre
Temperature ( °C)
Precipitation (mm)
Month
J F M A M J J A S O N D
25 20 15 10 5 0 -5 -10 -15
180 160 140 120 100 80 60 40 20 0

761 Fig. 3

762

763

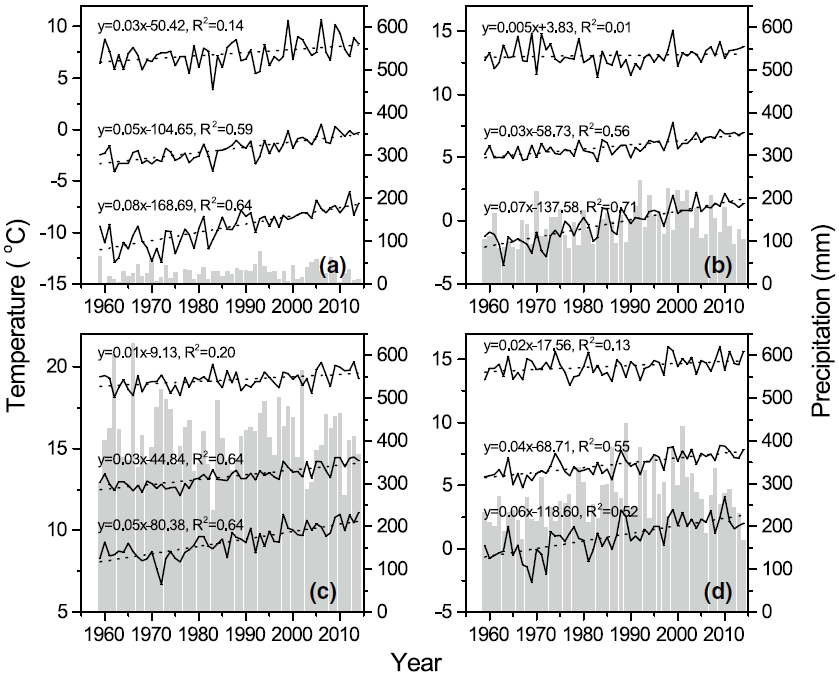


764

765

766 Fig. 4

767

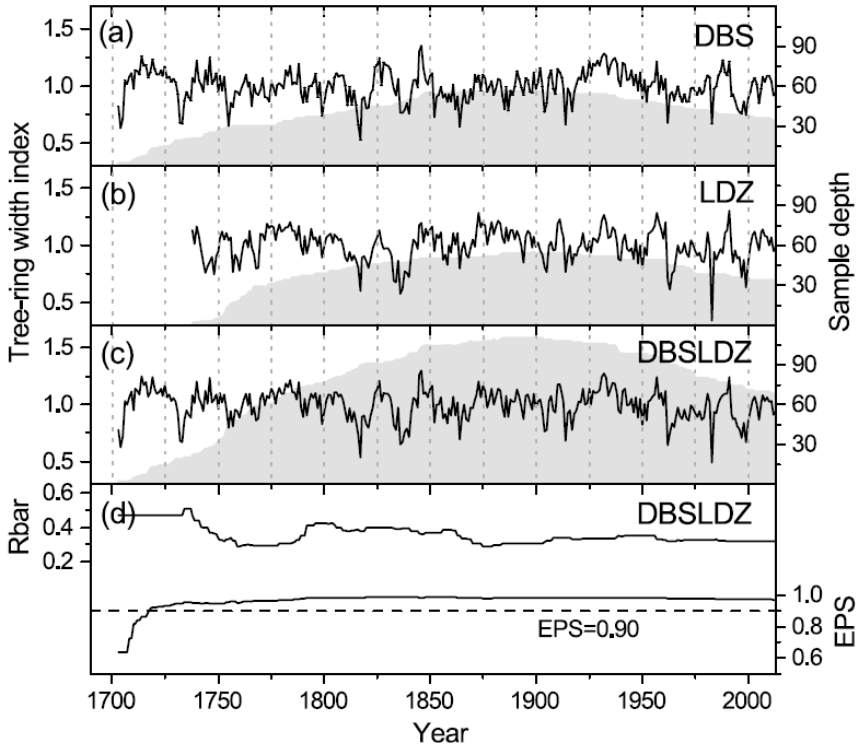


768

769

770

771 Fig. 5

772

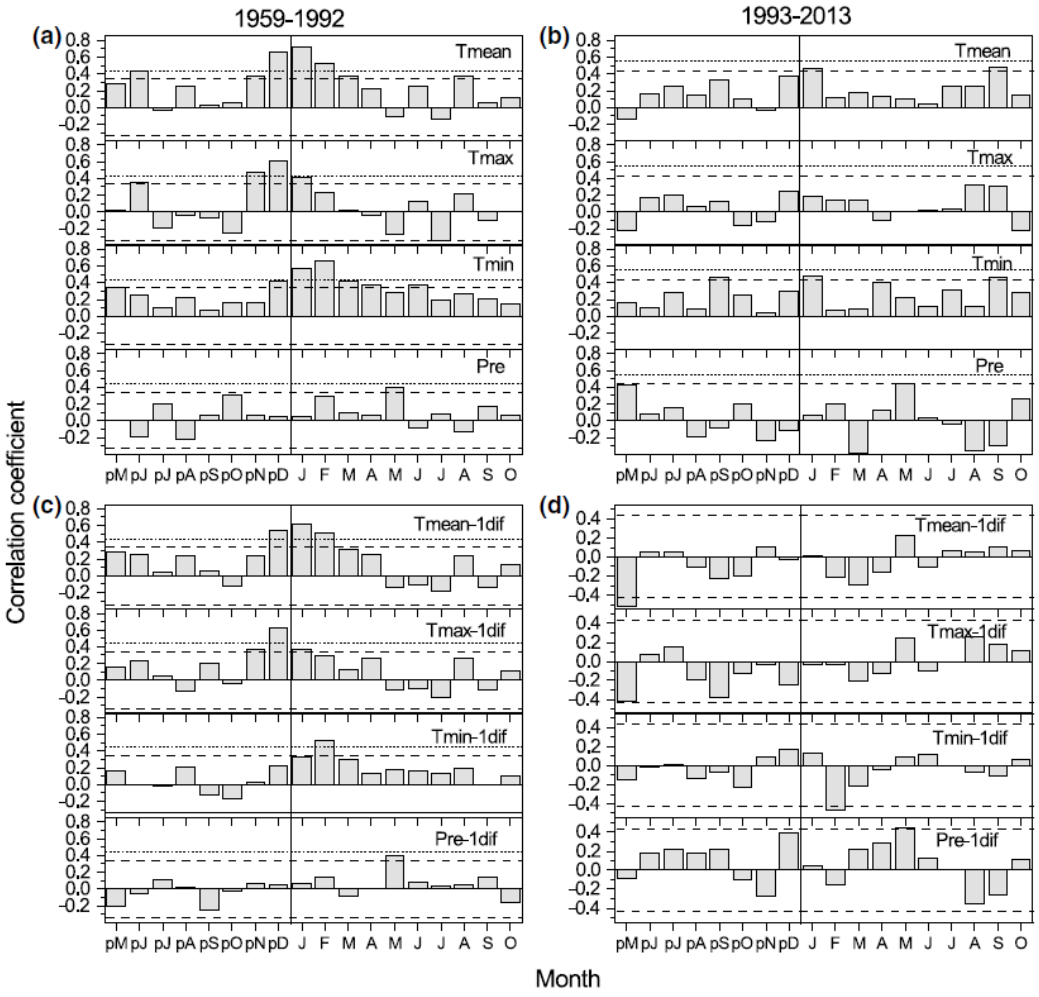


773

774

775 Fig. 6

776

777

778

779

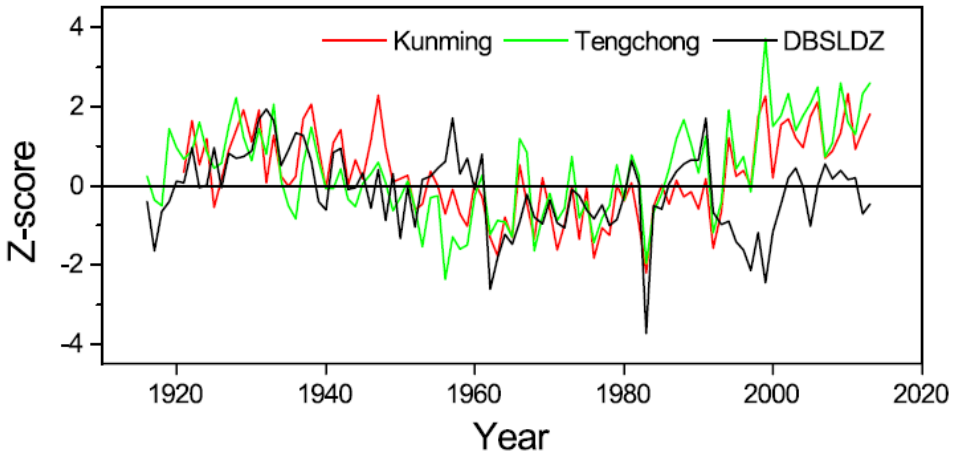


780

781

782 Fig. 7

783

784

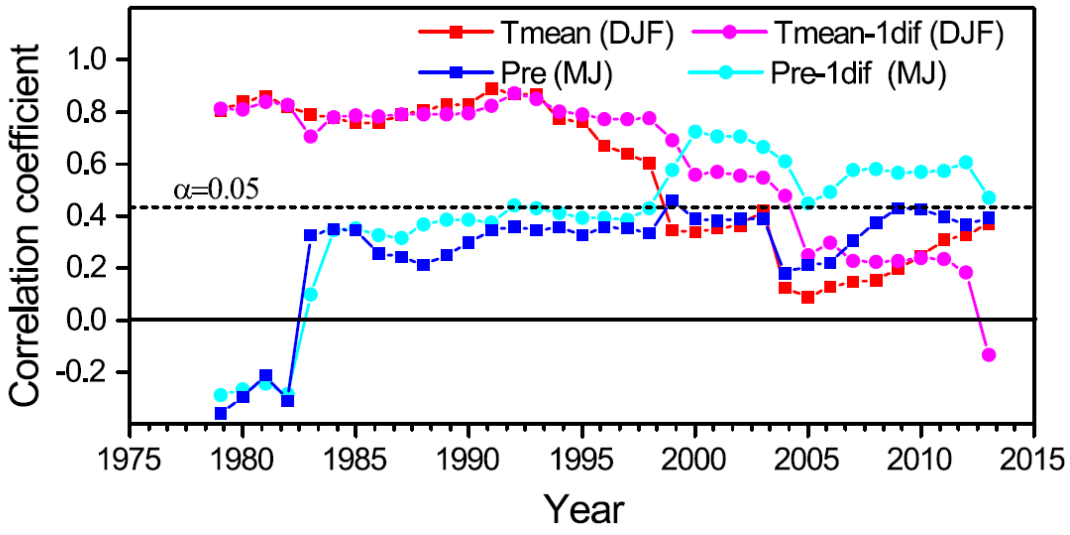


785

786 Fig. 8

787

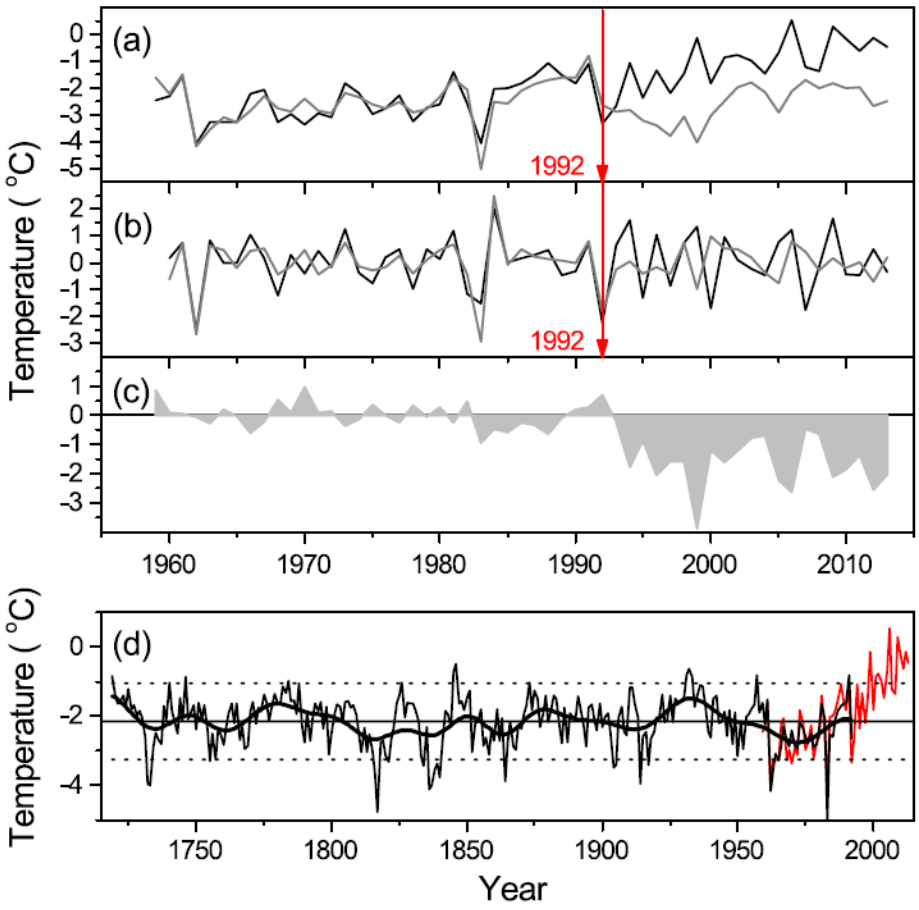


788

789

790 Fig. 9

791

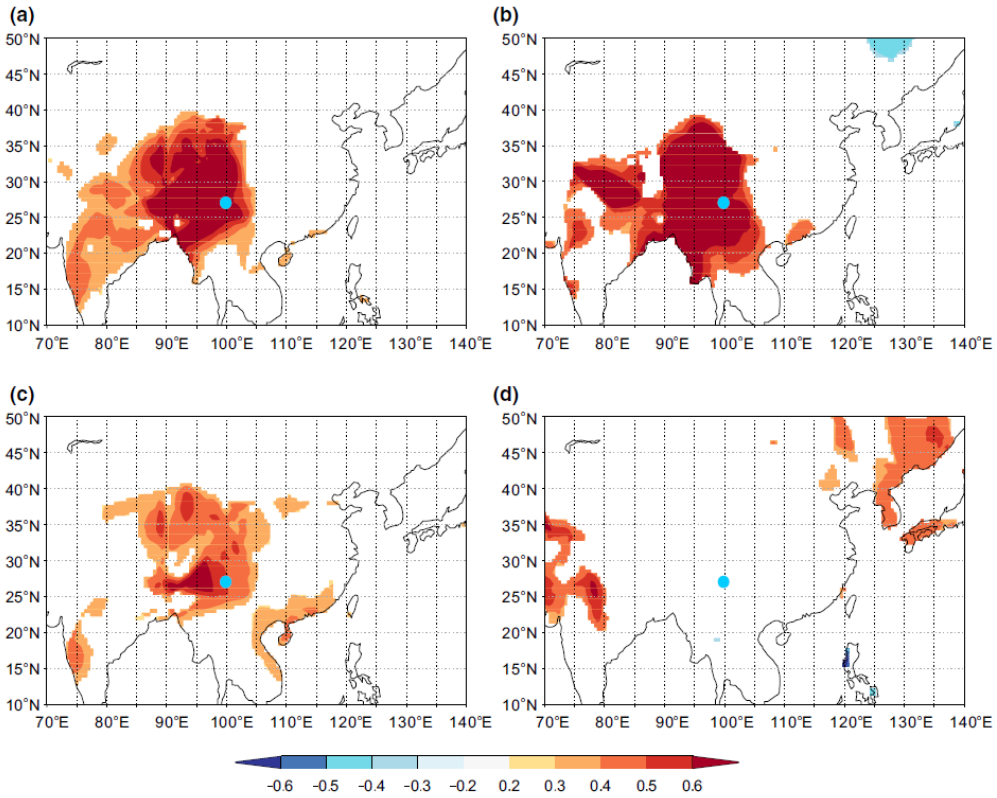


792

793

794 Fig. 10

795

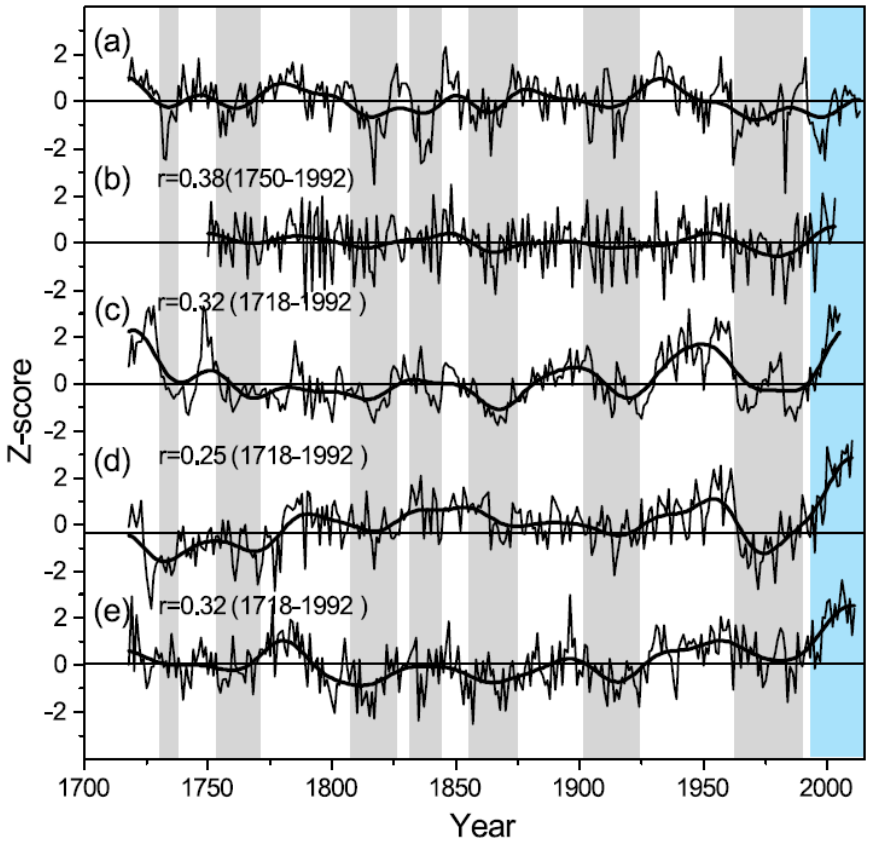


796

797

798 Fig. 11

799

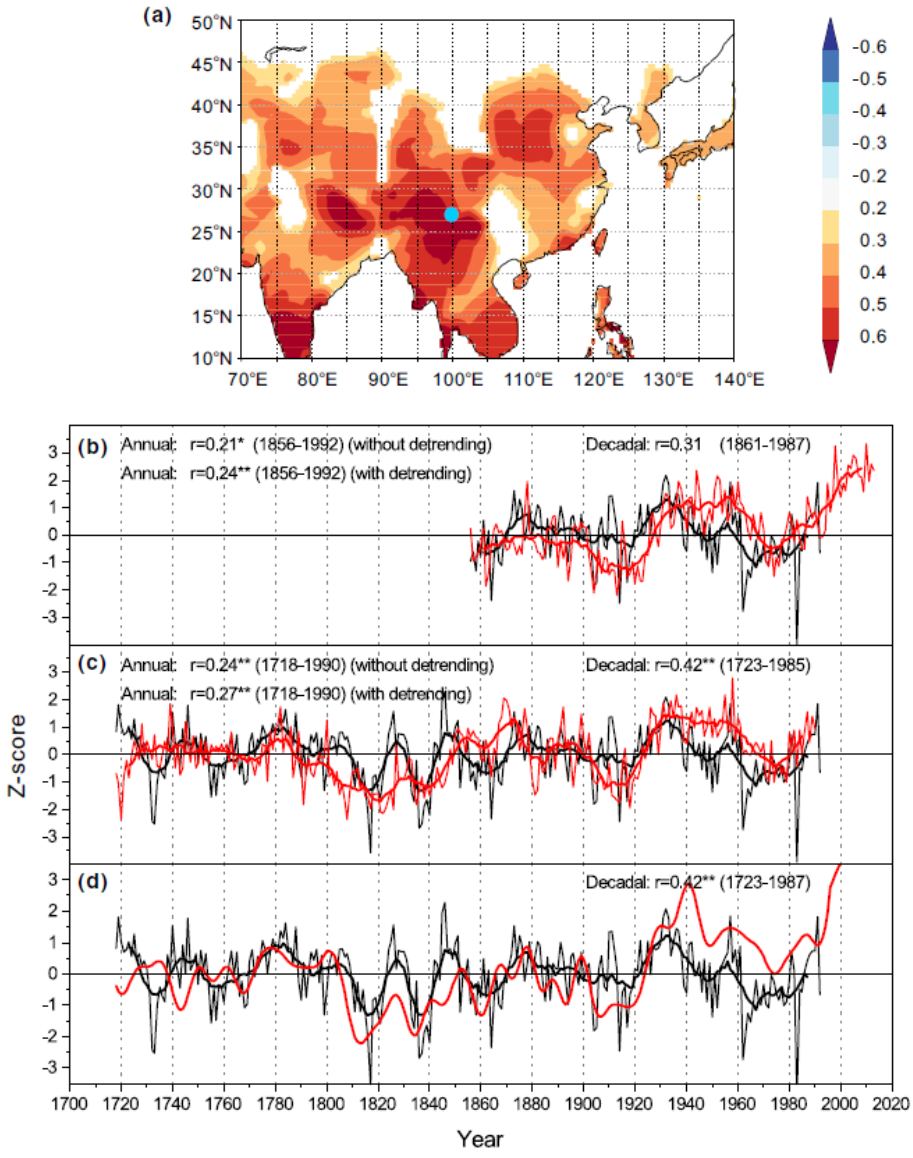


800

801